ChemPubSoc Europe

DOI: 10.1002/chem.201600207

CHEMISTRY
A European Journal
Full Paper

Structure–Property Relationships

Flavin Derivatives with Tailored Redox Properties: Synthesis, Characterization, and Electrochemical Behavior

Attila Kormányos,[a, b, c] Mohammad S. Hossain,[a] Ghazaleh Ghadimkhani,[a] Joe J. Johnson,[a] Csaba Janáky,[b, c] Norma R. de Tacconi,[a] Frank W. Foss, Jr.,[a] Yaron Paz,[d] and Krishnan Rajeshwar*[a]

Abstract: This study establishes structure–property relationships for four synthetic flavin molecules as bioinspired redox mediators in electro- and photocatalysis applications. The studied flavin compounds were disubstituted with polar substituents at the N1 and N3 positions (alloxazine) or at the N3 and N10 positions (isoalloxazines). The electrochemical behavior of one such synthetic flavin analogue was examined in detail in aqueous solutions of varying pH in the range from 1 to 10. Cyclic voltammetry, used in conjunction with hydrodynamic (rotating disk electrode) voltammetry, showed quasi-reversible behavior consistent with freely diffusing molecules and an overall global $2e^-$, $2H^+$ proton-coupled electron transfer scheme. UV/Vis spectroelectrochemical data was also employed to study the pH-dependent electrochemical behavior of this derivative. Substituent effects on the redox behavior were compared and contrasted for all the four compounds, and visualized within a scatter plot framework to afford comparison with prior knowledge on mostly natural flavins in aqueous media. Finally, a preliminary assessment of one of the synthetic flavins was performed of its electrocatalytic activity toward dioxygen reduction as a prelude to further (quantitative) studies of both freely diffusing and tethered molecules on various electrode surfaces.

Introduction

As part of a broader project on bioinspired electro- and photocatalyst assemblies,[1,2] we describe below the results of a study on the electrochemical behavior of four synthetic flavins in aqueous media. Flavins are biologically important yellow molecules with a common three-ring isoalloxazine structural motif, of which three natural analogues are well known: riboflavin, flavin mononucleotide (FMN), and flavin adenine dinucleotide (FAD) (Figure 1). All three molecules share the common feature of 7,8-dimethyl substitution of the benzene subnucleus but differ in the side chains at the N10 position. Additionally, lumiflavin, is a riboflavin analogue in which the ribotyl substituent at the N10 position is photochemically cleaved to a methyl group (Figure 1). The isoalloxazine moiety (particularly the bis-imine of the quinone-like core) forms the electroactive part of the molecules while the N10 substituents aid in apoprotein-cofactor binding and specificity.[3–5] The other substituents (at the C7 and C8, N1, N3, and N5 positions, Figure 1), as elaborated further in what follows, have direct effects on stability, solubility, pK_a, and redox potential.

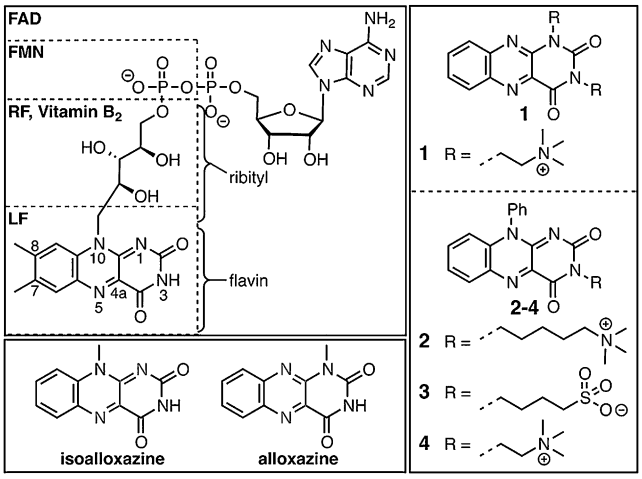

Figure 1. Synthetic flavins in the present study and their relationship to natural analogues. **RF** and **LF** stand for riboflavin and lumiflavin, respectively.

The electrochemical behavior of flavins, particularly riboflavin, FMN, and FAD but also lumiflavin, has been extensively

[a] A. Kormányos, M. S. Hossain, G. Ghadimkhani, J. J. Johnson, Prof. N. R. de Tacconi, Prof. F. W. Foss, Jr., Prof. K. Rajeshwar
Department of Chemistry and Biochemistry
University of Texas at Arlington, Texas, 76019 (USA)
E-mail: rajeshwar@uta.edu

[b] A. Kormányos, Prof. C. Janáky
Department of Physical Chemistry and Materials Science
University of Szeged, Szeged, 6720 (Hungary)

[c] A. Kormányos, Prof. C. Janáky
MTA-SZTE „Lendület" Photoelectrochemistry Research Group
Rerrich Square 1, Szeged, 6720 (Hungary)

[d] Prof. Y. Paz
Department of Chemical Engineering, Technion
Haifa 32000 (Israel)

Supporting information for this article is available on the WWW under http://dx.doi.org/10.1002/chem.201600207.

studied;[6–55] the early literature up to 1983 has been discussed in book chapters and review articles.[6–8] A wide range of electrode materials and supports were investigated in these studies. This corpus of literature work, however, has mostly focused on natural flavins (i.e., riboflavin, FAD, FMN) and much less is known about their synthetic counterparts. The few studies on synthetic flavins, on the other hand, were directed toward understanding substituent effects on redox potentials by theoretical and experimental means.[22,28,43,46] The present study, in contrast, differentiates itself from the extensive prior body of work on natural flavins by focusing on freely-diffusing synthetic flavin molecules, and their redox properties, especially from electrocatalysis and photocatalysis perspectives. Thus this study focuses on the reductive (i.e., cathodic) electrochemical behavior of four synthetic flavin derivatives in aqueous media.

The distinguishing side groups of riboflavin, FMN, and FAD (Figure 1) are also a potential source of instability for applications such as in fuel cells and in heterogeneous photocatalysis. Flavins **1**–**4** (Figure 1) were thus designed for enhanced redox stability and aqueous solubility over a broad pH range. Furthermore and, most importantly, these species avoid intramolecular proton-transfer events[22] stemming from the acidic N3 imide proton in the natural flavins during redox cycling.

Alloxazine **1** (Figure 1), the primary focus of this study, was selected because it has a more thermodynamically favorable interaction with dioxygen (O_2) after electrochemical reduction, in comparison to isoalloxazines **2**-**4**, which have more positive redox potentials. While all reduced flavin mimics are thermodynamically disposed to reduce O_2, initial electron transfer from reduced flavin to O_2 is the kinetic barrier to this interaction. In biological oxidoreductases, where constitutive formation of reactive oxygen species should be limited, the protein structure and environment serve to accelerate the redox process.[56,57] Furthermore, the relative synthetic ease with which two permanent cationic species can be installed in **1**, with comparison to the monoionic isoalloxazine systems, imparts excellent solubility over a wide range of pH.

While **1**–**4** are incompletely described as azaquinones (Figure 1, redox active bisimines), both species have resonance forms that contribute to an azaquinone, or quinone-like, system. Further, their redox properties are similar to the quinone systems, and changes in pK_as and relative redox potentials between alloxazines and isoalloxazines are related to the different alkylation sites, and consequently the relative protonation sites of the chemically reduced flavins (N1–H for isoalloxazines and N10–H for alloxazines). The nature of these Ns (N10, anilino- and N1, amido-) alters the electron density and distribution of the system in a predictable manner, resulting in a $>$150 mV negative shift in redox potentials for isomerization of the C=N double bond from the amido-N1 site to the aniline-N10 site. Such aspects are highlighted in the comparative voltammetry behavior of **1**–**4** presented in the following.

In line with the extreme versatility of voltammetry in its variant modes (linear sweep, cyclic, or hydrodynamic) for the electrochemical study of organic molecules,[57] this technique was primarily employed in the present study on **1**–**4** (Figure 1) in conjunction with UV/Vis spectroelectrochemical (SPEC) experiments[36,40,59] for mechanistic elucidations related to proton-coupled electron transfer (PCET). Important aspects related to PCET such as electron/proton stoichiometry and its sensitivity to solution pH, and proton starvation effects at the electrode-solution interface are discussed below, as is the influence of N-alkyl substitution (at N1/N10 and N3) on the redox potential of **1**-**4**. Finally, a preliminary assessment of the electrocatalytic properties of **1** for the dioxygen reduction reaction (ORR) is also presented. Follow-up collaborative studies will address tethered synthetic flavins on metallic and oxide semiconductor electrode supports, and their applicability to targeted multielectron transfer for ORR and solar water splitting.

Results and Discussion

Synthesis of aqueous soluble flavin derivatives

The preparation of ammonium-substituted flavins is detailed in Figure 2 and 3. Alloxazine (**5**) and N10-phenylisoalloxazine (**12**) core structures (Figures 2 and 3) were prepared as previously described.[60,61] N-alkylation to directly install quaternary ammonium groups was achieved by a rather specific procedure. Methylation of alloxazines at *N*-1 and *N*-3 is commonly achieved by standard single-step methods with methyl iodide.[67] However, the ammonium species pose obvious differences in reactivity and thermal stability compared to simpler haloalkanes. Figure 2 shows the major product (*N1*,*N3*-dimethylalloxazine, **8**) of one-step approaches to the desired products from commercially available halides **6** and **7**. Attempts to install an *N*,*N*-dimethylated substituent from compound **9** led us to intermolecular product **10** under a variety of one-pot conditions.

Quaternary ammonium containing flavins were successfully prepared by a simple two-step procedure from commercially available materials. Nucleophilic dipotassium alloxazine **11** was achieved by heating alloxazine with potassium carbonate in DMF. Subsequent treatment of the isolated salt with bromoalkyl ammonium species **6** in DMF produced the desired water-

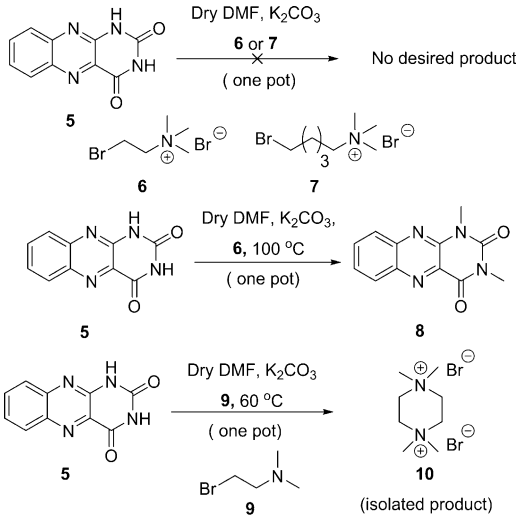

Figure 2. Outcome of single-step attempts to prepare desired flavin mimics.

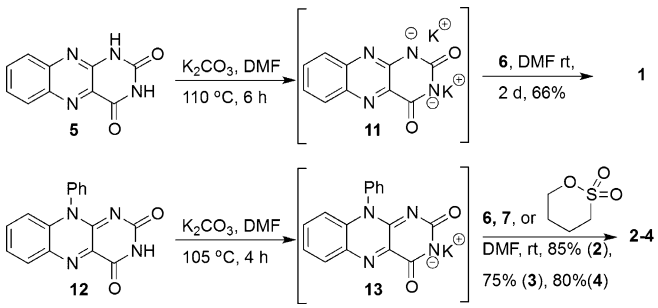

Figure 3. Derivatization of flavin salts with ammonium linkers.

soluble product, **1**. Formation of flavin salts in this manner was easily extended to N10-phenlyisoalloxazine derivatization to prepare isoalloxazines **2** and **4**, which bear varying carbon lengths. The potassium salt **13** was also used to generate the sulfonic acid modified flavin **3** by nucleophilic opening of butane sultone. The choice of K_2CO_3 as base was critical for the success of this two-step process. Hydroxides and alkoxides led to lower yields of the anionic flavins. Full experimental and characterization details are provided in the Supporting Information.

Electrochemical aspects—Survey CV experiments

Representative CV traces are contained in Figure 4a for **1** for a glassy carbon (GC) working electrode in pH 7 buffer at potential scan rates ranging from 20 to 300 mV s^{-1}. A single set of quasi-reversible waves were seen in the reductive regime (Figure 3a). These waves were diffusion-controlled as deduced from two trends: 1) The wave shapes and non-zero peak separation (i.e., the waves in the CV traces in Figure 4a were not sharp/symmetric without diffusion tails, and did not have 0 mV peak separation as expected for a surface-confined redox process;[62] 2) The Randles–Sevcik plots[63] in Figure 4b revealed a square-root potential scan rate (rather than linear) dependence of the peak current. Essentially similar CV behavior was observed for the polycrystalline Au working electrode surface (data not shown). It is important to underline that the behavior in Figure 4 for the GC surface, and trends from other experiments for both GC and Au surfaces (data not shown), were generally consistent with those expected for freely-diffusing flavin molecules in the aqueous media employed in this study.

Previous authors have described adsorption of riboflavin, FAD, and other *natural* flavin analogues for a variety of electrode surfaces including GC.[11, 14, 16–18, 20, 24, 30, 36, 48] These prior studies reveal that much less FAD was adsorbed on GC, Pt, and Au surfaces relative to the graphite case; the adsorbed layer was removed in these cases even with a single rinse. This trend is entirely consistent with the findings for **1** in this study for which negligible adsorption was seen on either GC or polycrystalline Au. Furthermore, the phosphate group of FAD, which is not present in **1**, is believed to be the major anchor on some electrode surfaces.[17]

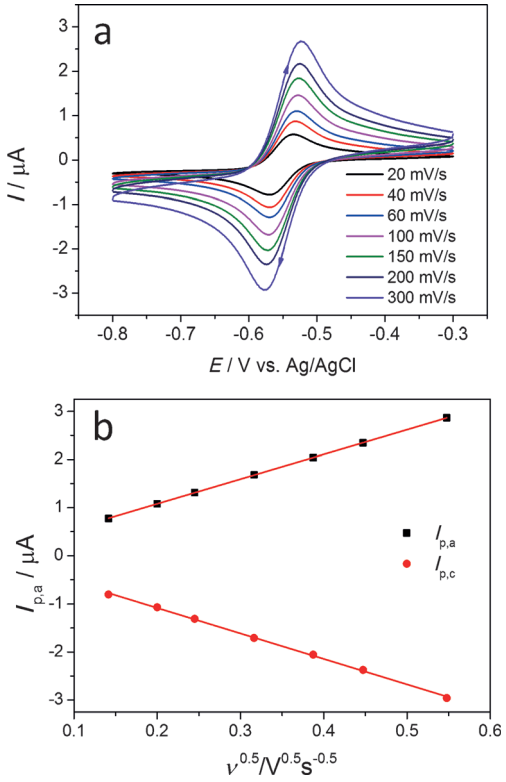

Figure 4. a) CV traces for the synthetic flavin derivative, **1** at a GC electrode surface as a function of potential scan rate in 0.1 M phosphate buffer solution (pH: 7). b) Plots of the peak current versus the square root of the potential scan rate constructed from the data in Figure 4a. The solid lines in Figure 4b are least-squares fits of the data points shown as circles or squares.

pH dependence of redox potentials for the synthetic flavin 1

The CV waves were pH-dependent for all the four synthetic derivatives (**1**–**4**) considered in this study, diagnosing that initial electron transfer was accompanied by proton transfer leading to a proton-coupled electron transfer (PCET) scheme (see below). Figure 5 contains CV traces for **1** at the GC electrode surface for buffered solutions of varying pH ranging from 3 to 10. The redox waves systematically shifted to more negative potentials as the pH was increased.

The electron/proton stoichiometry of the flavin reduction process can be probed by plotting the dependence of the reduction potential, E_{pc} versus solution pH; the results are shown in Figure S1, Supporting Information, for the buffered solutions. The slope of the plots (~-55 mV/pH unit) is consistent with that expected for a 2 e^-, 2 H^+ PCET process.

Note that 1 e^-, 1 H^+ stoichiometry (or for that matter, any pathway involving equal numbers of electrons and protons) would also have been consistent with observation of a (nernstian) −55 mV/pH unit slope value. Importantly, both our CV (e.g., Figure 5) and hydrodynamic (rotating disk electrode or RDE) voltammetry data (Figure 6) rule out that possibility. Figure 6a contains RDE data for a buffered solution of pH 9; Figure 6b contains Koutecky–Levich plots[63] constructed from these hydrodynamic voltammetry data along with two other plots derived from data on buffered solutions of pH 3 and 7

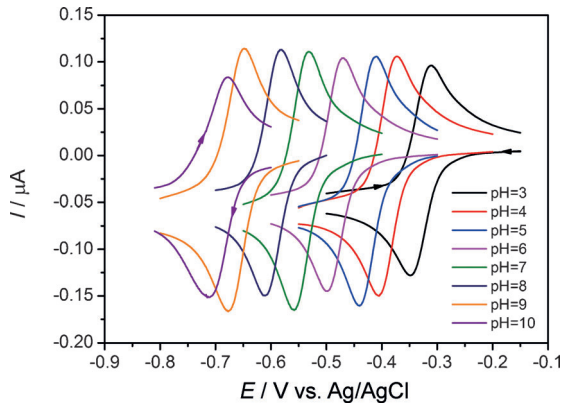

Figure 5. CV traces for the synthetic flavin derivative, **1** at a GC electrode surface as a function of pH in buffered aqueous media. See the Experimental Section for details.

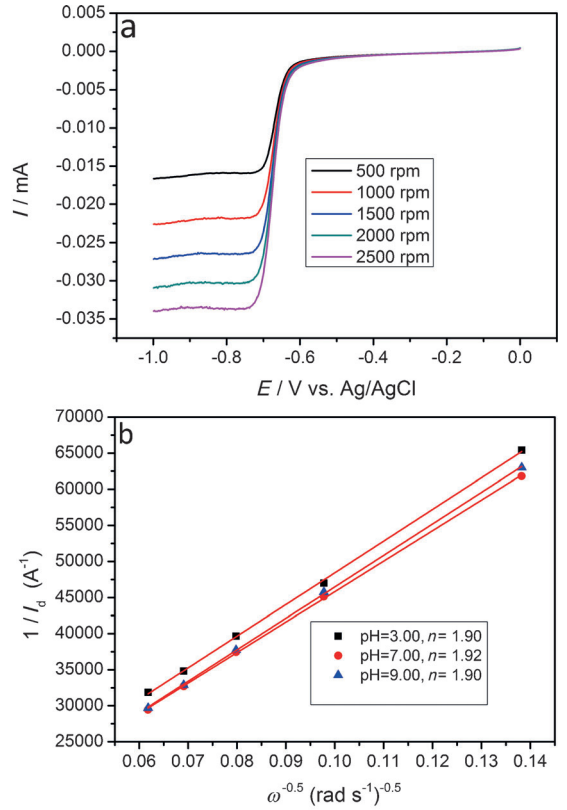

Figure 6. a) Hydrodynamic voltammograms for the synthetic flavin, **1** on a GC electrode surface in pH 9 buffered medium. b) Koutecky–Levich plots from RDE voltammetry data obtained at pH 3, 7, and 9 (see also Figure S2 in the Supporting Information).

(see also the Supporting Information, Figure S2). The electron stoichiometry values obtained from analyses of these plots are contained in Table 1. Values derived from the Randles–Sevcik plots (i.e., slopes of CV peak current versus square root of potential scan rate, c.f., Figure 4b and Figure S3, Supporting Information) are also contained in Table 1. The analyses in Table 2 provide further corroboration for our assertion that n is indeed close to 2; the computed diffusion coefficient (D) values are clearly unreasonable for a molecule of the size of flavin if an n value of 1 is assumed.

Table 1. Electron stoichiometry (n) calculated from the Koutecky-Levich and Randles-Sevcik plots.[a]

pH	3	7	9	
n (from RDE)	1.90	1.92	1.90	n (from RDE)
n (from CV)	–	1.83	–	n (from CV)

[a] See also Figure 4b, b, and Figure S3, Supporting Information. The diffusion coefficient value needed for these calculations was taken from Ref. [53].

Table 2. Calculated values for D if $n=1$.[a]

pH	3	7	9	
D/cm^2 s^{-1}	9.92E-6	1.014E-5	9.92E-6	D/cm^2 s^{-1}

[a] These are clearly unreasonable pointing to the fact that n cannot be 1 as assumed here. In fact, the computed D values would then be smaller than even that of anthraquinone, for example!

Interestingly, in unbuffered aqueous media, the pH dependence of E_{pc} is greatly attenuated in neutral solutions in an intermediate pH range that spans 4–7 (data not shown). When buffered solutions were utilized, the ~−55 mV/pH unit slope trend appeared over the entire pH range studied from 1 to at least 10 (Figure S1, Supporting Information). Factors in the invariance of E_{pc} with solution pH (as seen for unbuffered media in this study) can be understood in the light of a particularly elegant study on quinones.[64] An overall 2e$^-$, 2H$^+$ PCET scheme was accepted by these authors for buffered media for quinones in general.[64] According to these authors, however, a much better description of the overall reaction in unbuffered water was a 2e$^-$ electrochemical reduction scheme to make a strongly hydrogen-bonded quinone dianion. The latter was posited to exist in water as an equilibrium mixture of protonation states.[64] Strikingly, the $E_{1/2}$ versus pH plots presented by these authors for anthraquinone sulfonate showed lowered sensitivity or even insensitivity to pH for unbuffered solutions in the 4–8 pH range (cf., Figure 4 in ref. [64]).

Prior studies on electron/proton stoichiometry and the pH dependence of redox potentials are mostly confined to tethered natural flavin molecules on electrode support surfaces. Even in cases for which detailed data exist on pH-potential diagrams for molecules such as 7,8-dimethylisoalloxazine, FMN, FAD etc, these pertain to thin-layer electrochemical cell (thin-layer voltammetry) situations.[8,10] Notwithstanding these distinctions, the vast majority of the available literature on flavins is consistent with nernstian behavior in buffered solutions reverting to much lower slopes in unbuffered aqueous electrolyte situations.

UV/Visible spectroelectrochemical (SPEC) behavior of 1

Three distinct solution pH regimes centered at 3, 7, and 9 respectively were chosen for our aqueous-medium UV/Vis SPEC

experiments in this study. The choice of these pH values reflected simply the acidic, neutral, and basic pH regimes in the PCET scheme. The initial spectra of **1** at the three different pH values (in buffered solutions) were essentially the same, indicating that the oxidized form had similar electronic structure independent from its protonation level (Figure S4, Supporting Information). Figure 7 contains dynamic SPEC data, recorded during a CV measurement, in phosphate buffer solution adjusted to pH 3. The arrow directions in Figure 7 signal the growth (up) or decay (down) of the spectral bands during initial electroreduction of **1**.

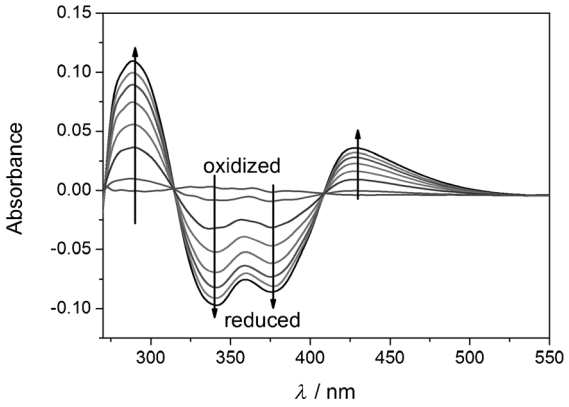

Figure 7. UV/Vis spectroelectrochemical data for **1** displayed as difference plots (see text) for a buffered solution with a pH value of 3. Potential scan conditions and other experimental details are given in the Experimental Section.

Figure 7 compares the evolution of the UV/Vis difference absorption (ΔA) spectra as a function of potential during a cyclic potential scan. A reference baseline spectrum, that is, one acquired at the rest potential for **1**, for pH 3 was subtracted from each successive potential-dependent spectrum. The arrows pointing down indicate bands disappearing while those pointing up correspond to new bands appearing.

The bands at 338 and 380 nm were attenuated on electroreduction of **1** while the longer-wavelength 435 nm band, together with the high energy band at 280 nm was enhanced. We note here that the overall pattern of the UV/Vis spectra was very similar for all three solution pH values (see Figure S5, Supporting Information, for pH 7 and 9). An important difference caused by the increasing pH is the gradual change in the ratio of absorbance measured at 280 and 435 nm, respectively. The relative intensity ($A_{\lambda=280}/A_{\lambda=435}$) of the band at 435 nm is decreasing in the series of increasing pH values from 3.0, through 2.3, to 0.9 (for pH 3, 7, and 9 respectively). Furthermore, at pH 9 the split of the band centered at 280 nm was observed into two new signatures centered at 275 and 288 nm, respectively.

The above observations suggest that the absorption bands of the differently protonated, fully reduced products can be assigned as follows: the highest-energy band (280 nm) belongs to the fully protonated H_2Fl, while the broad band centered at 435 nm belongs to both HFl^- and Fl^{2-}. We note here that similar trends were observed in earlier studies on natural flavins (such as lumiflavin, FMN, and flavoproteins) in aqueous solutions.[9,13,36]

Taken as a whole, the pH-dependent CV data and the SPEC data for **1** can be accommodated within the framework of the nine-member PCET scheme[65] contained in Figure 8. The assigned initial $2e^-$, $2H^+$ stoichiometry is consistent with rapid protonation of the product formed in the first reduction step. Indeed we fully anticipate that all the "vertical" (protonation/deprotonation) processes in the square scheme in Figure 8 are at equilibrium.

Cyclic voltammetry data on the other synthetic flavins (2-4)

Figure 9 compares CV traces for **1** with the corresponding data on **2**–**4** for the GC working electrode in buffered solutions.

To facilitate this comparison, the CV data in Figure 10 were acquired under identical experimental conditions (solution pH,

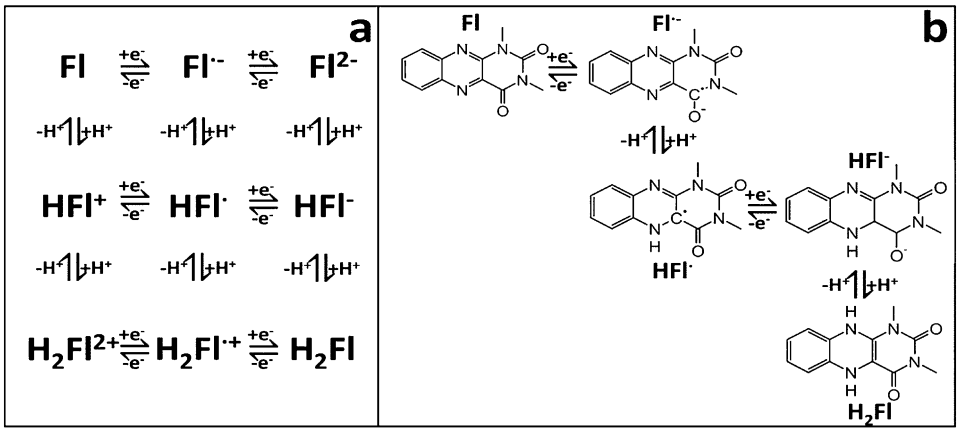

Figure 8. PCET in flavins in the reductive electrochemistry regime. The symbol "Fl", for example, denotes the starting synthetic flavin derivative (**1** in Figure 1) prior to electrochemical reduction ultimately to the $2e^-$, $2H^+$ reduced hydroquinone product, "H_2Fl". Other protonated and nonprotonated species involving the $1e^-$ and $2e^-$ electroreduction pathways are shown. UV/Vis spectroelectrochemical data for **1** displayed as difference plots (see text) for an unbuffered solution with initial pH value of 3. Potential scan conditions and other experimental details are given in the Experimental Section.

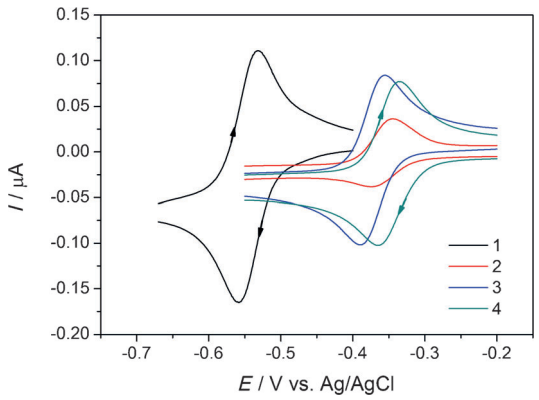

Figure 9. CV traces at GC electrodes in aqueous media for the four synthetic flavins, **1**–**4** in buffered electrolytes of pH 7. All the scans were run with the same electrode and under comparable potential scan rate and analyte concentration (see the Experimental Section) to facilitate direct comparison.

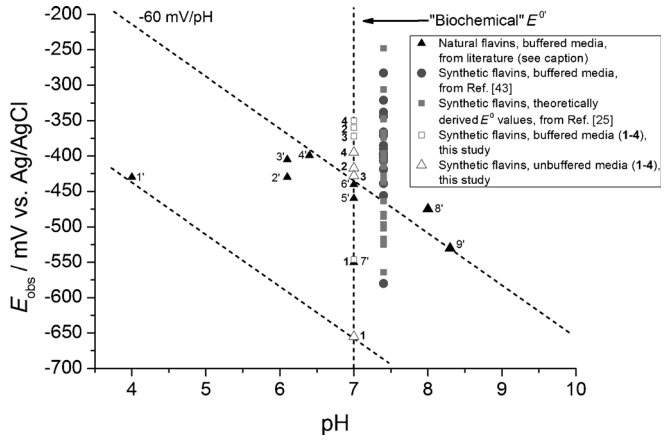

Figure 10. A scatter plot of reduction potentials (E_{obs}) as measured in this study for the synthetic flavins, **1**–**4** and comparison with selected literature data. Data on the compounds labeled **1′**–**9′** are culled from the literature on FAD using various buffers ranging in pH from 4 to 8.3: **1′**, **2′** (Ref. [11]), **3′** (Ref. [17]), **4′** (Ref. [38]), **5′** (Ref. [30]), **6′** (Ref. [42]), **7′** (Ref. [41]), **8′** (Ref. [12]), and **9′** (Ref. [34]). Note that E_{obs} is used in this plot (rather than E_{pc} as in Figure 5 above, for example) because other authors use either E^0 or $E^{0\prime}$ for the redox potentials in Refs. [25] and [43]. The differences between these variant redox potentials amount to only a few mV and will not significantly perturb the visualization in this plot. Refer also to the text for significance of the dashed vertical line and the two dashed lines with slopes of - 60 mV/pH unit. UV/Vis spectroelectrochemical data for **1** displayed as difference plots (see text) for an unbuffered solution with initial pH value of 3. Potential scan conditions and other experimental details are given in the Experimental Section.

potential scan rate, etc.). These data showed that **1** was electroreduced at a more negative potential relative to **2**–**4**.

The CV currents vastly differed for **1** relative to the other three synthetic compounds (**2**–**4**; Figure 9). This trend is attributed to variations in mass-transfer efficacy brought about by the extra phenyl substituents and hydrophobic character of the flavin molecule in **2**–**4** (cf., Figure 1). Note that hydrophobicity is crucially dependent on the N-alkyl substituents. In particular, the long-chain alkyl substituent in **2** renders considerable hydrophobicity to the molecule; presumably, the end result is sluggish mass transport leading to the lowest CV currents observed in this case relative to **1**, **3**, or **4**. Note also that the redox kinetics are markedly irreversible for **2** relative to the traces for the other three compounds. The CV currents were highest for **1**; this compound being the least hydrophobic of the four synthetic flavins examined here. It also has the highest solubility in water relative to **2**–**4**. Further aspects related to mass transport of **1**–**4** (and other synthetic flavins) are deferred to follow-up studies.

In general, shifts in the redox potentials of organic molecules can be rooted in structural or chemical factors that are: 1) intrinsic to the molecule, for example, internal electric field/inductive effects, conformational changes upon electron addition to the molecule, N-alkylation patterns, etc.; or 2) extrinsic, such as complexation with metal ions, solution substrates etc. We focus here only on the proclivity of synthetic flavin molecules to undergo electroreduction, and our ability to tweak their $E^{0\prime}$ (or E_{pc}) by N-alkyl substitution (as in **1**–**4**, Figure 1). Alkylation of a synthetic flavin molecule either at the N5 or N10 positions is known to shift its redox potential in a positive direction, as described in the introduction,[28,43] making it easier to be electroreduced. Because of stability issues associated with N5 substitution, however, previous authors[28] preferred to use N1–N10 ethylene-bridged derivatives instead for this purpose. Thus, 200–250 mV potential shifts (relative to a synthetic lumiflavin analogues) were observed in E_{pc} (or $E^{0\prime}$) as measured by CV and square-wave voltammetry (SWV).[28]

On the other hand, substitution at the N1- and N3-positions, in our hands, imparts a negative shift in E_{pc} (Figure 9) relative to the "parent" flavin (Figure 1) substituted only at the usual N10-position. Further, the protein environment surrounding the flavin moiety (in flavoenzymes, for example) can have a crucial effect on electron-transfer kinetics, and hence on the redox potentials. Ample precedence exists for the manifestation of such effects, especially for natural flavins in the bioelectrochemistry literature,[3–8] an aspect not germane, however, to the present study on synthetic flavins.

The nature of the permanently charged N3 substituents provide a smaller effect on E_{pc} (Figure 9, **2**–**4**). While linear comparisons of field effects (F) are unreliable for flexible saturated alkane linkers, the experimental trend for **2**–**4** E_{pc} values is consistent with the substituent effect (σ_{ij}) model provided by previous authors.[71] In this model $\sigma_{ij} = F/r_{ij}$, in which r_{ij} is the distance between a substituent (i) and a fixed site of reactivity (j). The field effect of Me_3N^+ ($F = 1.52$) is significantly more positive than SO_3^- ($F = 0.09$), which supports reduction of **2** and **4** at more positive potentials. The linker is shorter in **4** than **2** and **3**, predicting the E_{pc} trend of **4** > **2** > **3**. Though it must be reiterated that the distances r_{ij} are not known, the trend fits such a field-effect argument.

Figure 10 contains a scatter plot for the comparison of reduction potentials as measured in this study for the synthetic flavins **1**–**4** and comparison with selected literature data. The influence of medium pH can be accommodated by simply invoking Nernstian behavior (i.e., −60 mV/pH unit shift; see Figure 6 above and the two dashed lines with this slope in Figure 11). Alternatively, the pH influence can be ameliorated

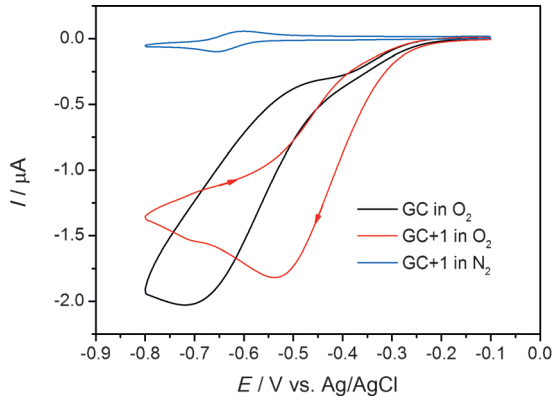

Figure 11. CV traces for GC electrodes in 0.1 M sodium sulfate (unbuffered, pH 7) in the presence of **1** in N_2-purged electrolyte (blue line). The corresponding traces for O_2 -purged electrolytes are with the presence (red line) and absence (black trace) of **1** in the electrolyte. Thus the blue and black traces represent control runs showing the intrinsic redox behavior of the flavin and the baseline electrocatalytic activity of the GC surface toward the ORR.

by using unbuffered electrolytes or by operating around the neutral pH 7 value (see vertical dashed line in Figure 10).

We note herein that redox potential values at the biologically relevant pH 7 have been traditionally regarded as the "formal potential"[66] by the biochemical (rather than the bioelectrochemical) community. Other than the data culled from this study on **1**–**4** in both buffered and unbuffered electrolytes, Figure 10 contains redox potential values computed by quantum-chemical calculations for synthetic flavins.[43] Also shown for comparison are values measured by CV for other synthetic flavins in HEPES buffer (pH 7.4) on a GC electrode.[25]

Further, the trends hold for buffered and unbuffered electrolytes equally well (Figure 10). Taking all the data together, this figure displays the full range of flavin redox potentials that has been achieved to date by synthetic alteration or by pH variation. Clearly, the manifold uses of these fully organic materials hint at their potential for functional (photo)electrocatalysis—a topic to be addressed in our ongoing follow-up studies.

Initial assessment of the electrocatalytic activity of 1 for the ORR

All the experiments described above, were performed in nitrogen-purged aqueous electrolytes. On the other hand, Figure 11 contains relevant CV traces for O_2-saturated 0.1 M sodium sulfate electrolyte (pH 7) for the GC electrode, in solutions without and with the synthetic flavin **1**. A control run for the N_2-saturated case is also shown for comparison in Figure 11.

These data bear all the hallmarks associated with classical homogeneous electrocatalysis:[58,62] 1) the CV currents are greatly enhanced (by a factor of ~10) in the presence of O_2 substrate in the solution; 2) the CV trace is shifted in the positive direction when **1** is present (relative to the control scan on GC in O_2-saturated supporting electrolyte); and 2) the redox waves associated with the electroreduction of **1** become irreversible in the presence of O_2 (Figure 11).

The preliminary data were presented here merely to underline that our synthetic flavins (such as **1**) do have the virtue of electrocatalytic activity toward solution substrates such as O_2. A fuller study affording quantitative assessments of electrocatalytic activity for O_2 and other substrates is in progress.

Conclusion

In summary, this study has attempted to fill the knowledge gap that existed on the mechanistic aspects of PCET for synthetic flavins in aqueous media. Hitherto such studies had mostly addressed: 1) Inductive effects associated with ET in these molecules (c.f., Figure 10) or 2) strategies for tethering natural flavins (and flavin analogues such as lumiflavin) on support matrices of interest, and subsequently characterizing these assemblies. Adsorption of flavins on electrode surfaces was also emphasized in these earlier studies, which almost exclusively focused on natural compounds.

In contrast, the present study, importantly, shows that much can be learnt about PCET from studies on the electrochemical behavior of synthetic flavins in aqueous media. Aqueous media, especially at pH values close to the neutral point are biologically relevant. After all, water is an excellent proton donor and its use for organic (or bioorganic) electrochemistry studies obviates the need for externally added proton donors. The absence of side groups such as those present in riboflavin, FMN, and FAD in the synthetic flavin analogues examined here (see Figure 1), greatly simplifies their pH-dependent electrochemical behavior.

More generally, this work demonstrates the utility of scatter plots (such as the one in Figure 10) for visualizing and examining underlying factors in redox potential shifts. This can be done in two (or more) dimensions; as shown in Figure 10, pH-induced shifts manifest in the lateral direction while other factors exert shifts in the vertical direction. Traditionally this latter topic has been the realm of physical organic chemists where interpretation of redox potential shifts in terms of linear free energy correlations between E^0 (or $E^{0'}$) with parameters such as the Hammett values σ, is commonplace. On the other hand, our scatter plot in Figure 10 has practical value for visualizing such dependencies, and for identifying factors (both intrinsic and extrinsic, see above) that influence redox potentials. The influence of N-alkyl substitution effects in **1**–**4** (Figure 1 and) is a case in point. Further, we point out that the use of such plots extends beyond flavins, and could include not only other organic molecules, but bioorganic and bioinorganic systems as well, and even solids.

Armed now with the basic electrochemical characterization of **1**–**4** (and other synthetic flavins in our hands), follow-up studies will address their electrocatalytic behavior in the freely-diffusing and tethered states as well their applicability in photocatalysis and solar water splitting.

Experimental Section

General

All chemicals were from commercial sources and were of the highest purity available. Deionized water (18 MΩ cm) was used in all cases for making solutions. Sodium sulfate (0.1 M concentration) was used as the supporting electrolyte for the voltammetry and SPEC experiments; the solutions were thoroughly purged with prepurified N_2 prior to use in all the cases unless otherwise specified. The (unbuffered) electrolyte solutions with variable pH in the 1–10 range were obtained simply by titration with the requisite amounts of sodium hydroxide or sulfuric acid in the 0.1 M sodium sulfate medium. Buffered solutions were prepared with phosphate (H_3PO_4/NaH_2PO_4 and NaH_2PO_4/Na_2HPO_4), acetate (CH_3COOH/CH_3COONa), and carbonate (Na_2CO_3/$NaHCO_3$) species as needed. All buffer concentrations were 0.1 M, and the pH was set at 3 with phosphoric acid/KH_2PO_4, 4, 5 with acetate and 6, 7, 8 with phosphate, and 9, 10 with carbonate species, respectively. The flavin derivatives (**1**–**4**, Figure 1) were synthesized by modified procedures.[67,68] Spectroscopic structure confirmation, purity (>99%), and other details are described in Supporting Information.

All reactions were performed under an argon atmosphere unless otherwise noted. Reagents and starting materials were purchased from commercial sources and used without any further purification. 500 MHz ^{1}H NMR and 125 MHz ^{13}C NMR were performed on a JOEL Eclipse Plus 500 NMR spectrometer. Chemical shifts were recorded in reference to residual solvent peaks ([D_6]DMSO = 2.50 and $CDCl_3$ = 7.26, D_2O = 4.90). IR spectra were recorded on a Bruker Alpha-P FTIR spectrometer by attenuated total reflectance on a diamond sample plate. Melting points of the compounds were obtained by using Mel-Temp II apparatus. TLC experiments were performed on EMD Merck F254, 250 mm thickness.

Electrochemical experiments were performed with a conventional three-electrode cell and glassy carbon (GC) working electrodes for CV. A few CV experiments were also performed on a polycrystalline Au working electrode (EDAQ, 1 mm diameter, part no. ET076–1) for comparison (data not shown below). A CH Instruments Model 600C potentiostat/waveform generator was used for CV. The GC disk electrode (BASi, 2.0 mm diameter) was polished with alumina slurry (Buehler, 0.05 μm) to mirror finish, followed by rinsing with doubly distilled deionized water. A Pt wire was used as the counter electrode for CV; all working electrode potentials below were measured with respect to a Ag/AgCl/KCl (satd.) reference electrode. The potential scan rate was 20 mV s^{-1} unless otherwise mentioned, and the nominal flavin derivative concentration in the supporting electrolyte (or buffer) was 0.1 mM.

Hydrodynamic voltammetry measurements were performed with a glassy carbon working electrode (Pine Instruments, geometric area = 0.196 cm^2). For electrode rotation, a Pine Instruments MSR rotor was used. The electrode surface cleaning procedure was the same as used above. A Pt wire was used as the counter electrode and Ag/AgCl/satd. KCl served as the reference electrode.

Spectroelectrochemical (SPEC) experiments utilized a diode array spectrometer (Hewlett–Packard Model 8453) equipped with a custom-built quartz thin layer cell; UV/V spectra were acquired in the transmission mode over a ~250–600 nm wavelength range. A gold mesh was used as the working electrode for SPEC experiments. Further details of the assembly/instrumentation, the Au gauze electrode and its pretreatment, and the thin-layer SPEC cell are given elsewhere.[69,70] The flavin derivative concentration in these experiments was 1.0 mM, in buffered solutions (pH 3, 7, and 9) and the potential was cyclically scanned at 5 mV s^{-1}. The counter electrode (a Pt wire) and a miniature Ag/AgCl/KCl (satd) reference electrode were laterally placed in a quartz optical cuvette next to the thin-layer SPEC cell compartment. The top part of the SPEC cell compartment was sealed with an airtight Teflon stopper with drilled perforations for electrode leads and solution degassing connectors as needed. All voltammetry, SPEC, and other electrochemical experiments were conducted at the ambient laboratory temperature (20 ± 2 °C).

Acknowledgements

Partial funding support for this work from the National Science Foundation, CHE-1303803 and CHE-0840509 (CRIF: MU), and from the University of Texas at Arlington is acknowledged. This research was also supported by the Hungarian National Development Agency in the framework of TÁMOP 4.2.4A/2-11-1-2012-001 "National Excellence Program-Elaborating and operating an inland student and research personal support system" key project. Finally, we thank two anonymous reviewers for constructive criticisms of an earlier manuscript version.

Keywords: cyclic voltammetry · hydrodynamic voltammetry · proton-coupled electron transfer · riboflavin mimics

[1] K. Rajeshwar, W. Chanmanee, *Electrochim. Acta* **2012**, *84*, 96–102.
[2] K. Rajeshwar, C. Janaky, W.-Y. Lin, D. A. Roberts, W. A. Wampler, *J. Phys. Chem. Lett.* **2013**, *4*, 3468–3478.
[3] C. Walsh, *Acc. Chem. Res.* **1980**, *13*, 148–155.
[4] G. Dryhurst, K. M. Kadish, F. Scheller, F. Renneberg in *Biological Electrochemistry, Vol. 1*, Academic Press, New York **1982**.
[5] A. M. Edwards in *Flavins: Photochemistry and Photobiology*, Royal Society of Chemistry, **2006**, Chapter 1, pp. 1–11.
[6] B. Janik, P. J. Elving, *Chem. Rev.* **1968**, *68*, 295–319.
[7] G. Dryhurst in *Electrochemistry of Biological Molecules*, Academic Press: New York, **1977**, Chapter 7, pp. 365–389.
[8] O. S. Ksenzhek, S. A. Petrova, *Bioelectrochem. Bioenerg.* **1983**, *11*, 105–127.
[9] S. Ghisla, V. Massey, J-M. Lhoste, S. G. Mayhew, *Biochemistry* **1974**, *13*, 589–597.
[10] O. S. Ksenzhek, S. A. Petrova, I. D. Pinielle, *Bioelectrochem. Bioenerg.* **1979**, *6*, 405–412.
[11] L. Gorton, G. Johansson, *J. Electroanal. Chem.* **1980**, *113*, 151–158.
[12] O. Miyawaki, L. B. Wingrad Jr., *Biochim. Biophys. Acta* **1985**, *838*, 60–68.
[13] J. H. Reeves, K. Weiss, *J. Electroanal. Chem.* **1987**, *217*, 65–78.
[14] V. I. Birss, H. Elzanowska, R. A. Turner, *Can. J. Chem.* **1988**, *66*, 86–96.
[15] R. Male, M. A. Samotowka, R. D. Allendoerfer, *Electroanalysis* **1989**, *1*, 333–339.
[16] M. M. Kamal, H. Elzanowska, M. Gaur, D. Kim, V. I. Birss, *J. Electroanal. Chem.* **1991**, *318*, 349–367.
[17] H. Shinohara, M. Gratzel, N. Vlachopoulos, M. Aizawa, *Bioelectrochem. Bioenerg.* **1991**, *26*, 307–320.
[18] V. I. Birss, A. S. Hinman, C. E. McGarvey, J. Segal, *Electrochim. Acta* **1994**, *39*, 2449–2454.
[19] Y. Wang, G. Zhu, E. Wang, *Anal. Chim. Acta* **1997**, *338*, 97–101.
[20] V. I. Birss, S. Guha-Thakurta, C. E. McGarvey, S. Quach, P. Vanysek, *J. Electroanal. Chem.* **1997**, *423*, 13–21.
[21] M. J. Barber, A. J. Trimboli, S. Nomikos, E. T. Smith, *Arch. Biochem. Biophys.* **1997**, *345*, 88–96.
[22] A. Niemz, J. Imbriglio, V. M. Rotello, *J. Am. Chem. Soc.* **1997**, *119*, 887–892.
[23] L. T. Kubota, L. Gorton, A. Roddick-Lanzilotta, A. J. McQuillan, *Bioelectrochem. Bioenerg.* **1998**, *47*, 39–46.
[24] C. McGarvey, S. Beck, S. Quach, V. I. Birss, H. Elzanowska, *J. Electroanal. Chem.* **1998**, *456*, 71–82.

[25] J. J. Hasford, C. J. Rizzo, *J. Am. Chem. Soc.* **1998**, *120*, 2251 – 2255. See also references therein.
[26] K. J. Stine, D. M. Andrauskas, A. R. Khan, P. Forgo, V. T. D'Souza, J. Liu, R. M. Friedman, *J. Electroanal. Chem.* **1999**, *472*, 147 – 156.
[27] N. Choy, K. C. Russell, J. C. Alvarez, A. Fider, *Tetrahedron Lett.* **2000**, *41*, 1515 – 1518.
[28] W. S. Li, N. Zhang, L. M. Sayre, *Tetrahedron* **2001**, *57*, 4507 – 4522.
[29] M. Zayats, E. Katz, I. Willner, *J. Am. Chem. Soc.* **2002**, *124*, 2120 – 2121.
[30] R. Garjonyte, A. Malinauskas, L. Gorton, *Bioelectrochemistry* **2003**, *61*, 39 – 49.
[31] A. C. Pereira, A. de S. Santos, L. T. Kubota, *J. Colloid Interface Sci.* **2003**, *265*, 351 – 358.
[32] Y. N. Ivanova, A. A. Karyakin, *Electrochem. Commun.* **2004**, *6*, 120 – 125.
[33] E. V. Milsom, H. R. Perrott, L. M. Peter, F. Marken, *Langmuir* **2005**, *21*, 9482 – 9487.
[34] K.-C. Lin, S.-M. Chen, *J. Electroanal. Chem.* **2005**, *578*, 213 – 222.
[35] G. Nöll, E. Kozma, R. Grandori, J. Carey, T. Schodl, G. Hauska, J. Daub, *Langmuir* **2006**, *22*, 2378 – 2383.
[36] C. Bonazzola, G. Gordillo, *J. Electroanal. Chem.* **2007**, *599*, 356 – 366.
[37] S. A. Kumar, S.-M. Chen, *J. Mol. Catal. A* **2007**, *278*, 244 – 250.
[38] S. A. Kumar, S.-M. Chen, *Sens. Actuators B* **2007**, *123*, 964 – 977.
[39] S. Ashok Kumar, P.-H. Lo, S.-M. Chen, *Nanotechnology* **2008**, *19*, 255501 – 255507.
[40] G. Nöll, *J. Photochem. Photobiol. A* **2008**, *200*, 34 – 38.
[41] H. Wei, S. Omanovic, *Chem. Biodiversity* **2008**, *5*, 1622 – 1639.
[42] A. Salimi, R. Hallaj, H. Mamkhezri, S. M. T. Hosaini, *J. Electroanal. Chem.* **2008**, *619 – 620*, 31 – 38.
[43] X.-L. Li, Y. Fu, *Theochem. J. Mol. Struc.* **2008**, *856*, 112 – 118.
[44] M. Bartosik, V. Ostatna, E. Palecek, *Bioelectrochemistry* **2009**, *76*, 70 – 75.
[45] A. Chatterjee, J. S. Foord, *Diamond Relat. Mater.* **2009**, *18*, 899 – 903.
[46] V. Sichula, Y. Hu, E. Mirzakulova, S. F. Manzer, S. Vyas, C. M. Hadad, K. D. Glusac, *J. Phys. Chem. B* **2010**, *114*, 9452 – 9461.
[47] H. Wei, H. Tan, Y. Zeng, *Phys. Chem. Liq.* **2010**, *48*, 708 – 722.
[48] L. B. Avalle, L. Valle, *J. Electroanal. Chem.* **2011**, *662*, 288 – 297.
[49] E. Mirzakulova, R. Khatmullin, J. Walpita, T. Corrigan, N. M. Vargas-Barbosa, S. Vyas, S. Oottikkal, S. F. Manzer, C. M. Haddad, K. D. Glusac, *Nat. Chem.* **2012**, *4*, 794 – 801.
[50] S. Nellaiappan, A. S. Kumar, *Electrochim. Acta* **2013**, *109*, 59 – 66.
[51] R. Ruinatscha, K. Buehler, A. Schmid, *J. Mol. Catal. B* **2014**, *103*, 100 – 105.
[52] J. M. Goran, S. M. Mantilla, K. Stevenson, *Anal. Chem.* **2013**, *85*, 1571 – 1581.
[53] S. L. J. Tan, J. M. Kan, R. D. Webster, *J. Phys. Chem. B* **2013**, *117*, 13755 – 13766.
[54] E. T. Smith, C. A. Davis, M. J. Barber, *Anal. Biochem.* **2003**, *323*, 114 – 121.
[55] M. Cable, E. T. Smith, *Anal. Chim. Acta* **2005**, *537*, 299 – 306.
[56] V. Massey, *J. Biol. Chem.* **1994**, *269*, 22459 – 22462.
[57] G. Gadda, *Biochemistry* **2012**, *51*, 2662 – 2669.
[58] J-M Saveant IN *Elements of Molecular and Biomolecular Electrochemistry*, Wiley-Interscience: Hoboken, NJ, **2006**.
[59] S. Vogt, M. Schneider, H. Schäfer-Eberwein, G. Nöll, *Anal. Chem.* **2014**, *86*, 7530 – 7535.
[60] K. Bergstad, J. E. Backvall, *J. Org. Chem.* **1998**, *63*, 6650 – 6655.
[61] G. Singh, R. Singh, S. Singh, *J. Chem. Res.* **2005**, *11*, 719 – 723.
[62] R. W. Murray in *Electroanalytical Chemistry, Vol. 13*, (Ed.: A. J. Bard), Marcel Dekker Inc.: New York **1984**, pp. 191 – 368.
[63] A. J. Bard, L. R. Faulkner in *Electrochemical Methods*, Wiley: New York **2001**, Chapters 6 and 9, pp. 226,331.
[64] M. Quan, D. Sanchez, M. F. Wasylkiw, D. K. Smith, *J. Am. Chem. Soc.* **2007**, *129*, 12847 – 12856.
[65] E. Laviron, *J. Electroanal. Chem.* **1984**, *169*, 29 – 46.
[66] See for example, D. C. Harris in *Quantitative Chemical Analysis*, W. H. Freeman and Co: New York, NY **2007**, Chapter 14, pp. 288.
[67] S. Chen, M. Hossain, F. W. Foss Jr., *Org. Lett.* **2012**, *14*, 2806 – 2809.
[68] S. Chen, F. W. Foss Jr., *Org. Lett.* **2012**, *14*, 5150 – 5153.
[69] N. R. de Tacconi, R. O. Lezna, R. Chitakunye, F. M. MacDonnell, *Inorg. Chem.* **2008**, *47*, 8847 – 8858.
[70] R. Konduri, N. R. de Tacconi, K. Rajeshwar, F. M. MacDonnell, *J. Am. Chem. Soc.* **2004**, *126*, 11621 – 11629.
[71] M. J. S. Dewar, P. J. Grisdale, *J. Am. Chem. Soc.* **1962**, *84*, 3548 – 3553.

Received: January 15, 2016
Published online on ■■ ▮▮, 0000

FULL PAPER

Structure–Property Relationships

*A. Kormányos, M. S. Hossain, G. Ghadimkhani, J. J. Johnson, C. Janáky, N. R. de Tacconi, F. W. Foss, Jr., Y. Paz, K. Rajeshwar**

■■ – ■■

Flavin Derivatives with Tailored Redox Properties: Synthesis, Characterization, and Electrochemical Behavior

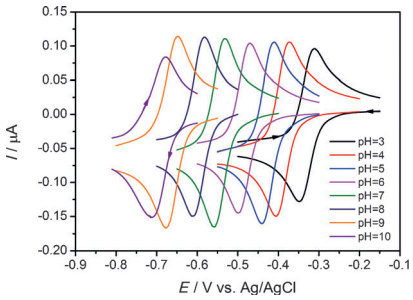

Substituent effects on the redox behavior of synthetic flavins were compared and contrasted for four synthetic flavin molecules as bioinspired redox mediators in electro- and photocatalysis applications. Structure–property relationships were established and visualized within a scatter plot framework (see figure) to afford comparison with prior knowledge on mostly natural flavins in aqueous media.